Standard Article

Thermodynamic modelling of a stratified charge spark ignition engine

Jamie Karl Smith[1] , **Phil Roberts[2], Alexandros Kountouriotis[3],
David Richardson[2], Pavlos Aleiferis[3] and Daniel Ruprecht[1]**

Abstract
Combustion of a charge with spatially and temporally varying equivalence ratio in a spark ignition engine was modelled using the Leeds University Spark Ignition Engine quasi-dimensional thermodynamic code. New sub-models have been integrated into Leeds University Spark Ignition Engine that simulate the effect of burnt gas expansion and turbulent mixing on an initial equivalence ratio distribution. Realistic distribution functions were used to model the radially varying equivalence ratio. The new stratified fuel model was validated against experimental data, showing reasonable agreement for both the pressure trace and percentage heat released. Including the effect of turbulent mixing was found to be important to reproduce the trend in the differences between the stratified and homogeneous simulations.

Introduction

In a bid to meet the latest government regulations on pollution and consumer demands, engine manufacturers are continually looking at new combustion strategies that consume less fuel and/or produce fewer emissions. In addition, the automotive industry are also looking to reduce production and design costs.

A potential way of improving the thermal efficiency of the working cycle is by adapting stratified fuel injection, rather than 'traditional' homogeneous fuel injection. The benefits of stratified charge include[1] (1) reduced pumping losses due to unthrottled part-load operation, (2) decreased heat loss to cylinder walls and (3) an increase in compression ratio due to lower end gas temperatures associated with stratified combustion. Lower-end gas temperatures also reduce the chance of autoignition, although typically the stratified charge engines run under conditions in which the probability of autoignition is already small.

Disadvantages of fuel stratification are an increase in NOx emissions when compared to a homogeneous lean burn engine, as well as control of the fuel spray to ensure the fuel arrives at the spark plug at the correct time. Stratification also causes the exhaust temperature to be cooler than that of a homogeneous lean burn engine, therefore consideration must be given to the aftertreatment operating at these low temperatures.[2]

However, Wirth et al.[3] found that fuel stratification is a viable combustion strategy at low load, showing a decrease in both fuel consumption and NOx emissions.

Computational models save prototyping costs with respect to drafting, manufacturing and assembly of parts, and eliminating the time taken to produce these prototypes. Two commonly used types of computational modelling strategies are thermodynamic quasi-dimensional modelling and computational fluid dynamics (CFD). Thermodynamic modelling uses the laws of thermodynamics to determine parameters such as the in-cylinder pressure and temperature, whereas CFD modelling solves the in-cylinder processes as a fluid flow using defined boundary conditions. The quasi-dimensional model is not resolved spatially, other than the location of the flame radius for a given time-step. In contrast, CFD models physical processes in three dimensions, resolving turbulent flow, fuel injection, and combustion. The advantages of using

[1]School of Mechanical Engineering, University of Leeds, Leeds, UK
[2]Jaguar Land Rover Powertrain Research, Coventry, UK
[3]Imperial College London, London, UK

Corresponding author:
Jamie Karl Smith, School of Mechanical Engineering, University of Leeds, Woodhouse Lane, Leeds LS2 9JT, West Yorkshire, UK.
Email: ed11j5s@leeds.ac.uk

thermodynamic quasi-dimensional codes as opposed to CFD is run time, with the typical run time of a thermodynamic code measured in minutes or seconds, compared to CFD having run times measured in hours, days or even months. Thermodynamic models are routinely used to analyse homogeneous combustion but have not yet been widely adapted for stratified charges.

Fuel stratification is reserved for direct injection (DI) spark ignition (SI) engines adapting late injection timing, which does not give the fuel–air mixture the time needed to perfectly mix and become homogeneous. So far, modelling of stratified charge and the effects of late injection have been predominantly carried out using CFD.[4–9] However, some research exists into quasi-dimensional stratified fuel models.[10–13] For example, the stratified model developed by Aghdam[10] used a radially varying equivalence ratio. The equivalence ratio distributions were modelled by either a linear or parabolic function. However experimental examples showed that both are not representative of a realistic distribution.[14,15] Aghdam's model is the only example that accounts for the expansion of burned gas assuming a cylindrically propagating flame.

The model developed by Schmid et al.[11] uses an injection model as opposed to an equivalence ratio distribution. It also models the mixing using a mass flow equation, with the turbulent root mean squared (RMS) velocity defined as the mass flow velocity. The mixing models the transition from fuel rich to fuel lean through stoichiometric conditions. To do this, three separate zones are constructed for the unburned gas, as opposed to a continuous distribution of the charge. The combustion is modelled in two stages with an initial spherical propagation before the second phase toroidal burning. Burned gas expansion is neglected.

The work by Sjeric et al.[12] utilised a fractal combustion model with an equivalence ratio distribution that varied with respect to the mass fraction burned. Both the effect of mixing and burned gas expansion were neglected. Aliramezani et al.[13] investigated a partially stratified charge of hydrogen and methane under lean conditions. It is not clearly stated how the distribution of fuel is calculated and the effect of burned gas expansion and turbulent mixing of the stratified charge is not mentioned.

No experimental validation was provided in the works by Aghdam[10] and Sjeric et al.[12] The work by Aliramezani et al.[13] was validated for the indicated mean effective pressure (IMEP) and brake-specific fuel consumption (BSFC). Neither metric is indicative of how stratification changes combustion over the course of a cycle. Schmid et al.[11] have validated their model for both the pressure trace and burn rate with good agreement.

This article describes and validates a novel thermodynamic model for stratified combustion. The model is new in several ways: it uses a realistic radially resolved initial distribution for the equivalence ratio, it includes a new physical sub-model that takes into account the

effect of turbulence on mixing the fuel–air charge distribution and it contains a modified burned gas expansion effect to simulate a spherically propagating flame. The inclusion of the turbulent mixing is necessary to simulate the physical processes that occur within the engine. An existing quasi-dimensional homogeneous combustion code is modified in this article to accommodate stratified fuel modelling. The model is validated against experimental data for both the pressure trace profile and for the rate of heat released.

Combustion code

The Leeds University Spark Ignition Engine (LUSIE) is a quasi-dimensional thermodynamic predictive combustion code. It predicts thermodynamic processes in both two- and four-stroke engines. LUSIE iteratively models the closed part of the combustion cycle, neglecting the intake and exhaust processes. The model is classed as quasi-dimensional as it separates the burned and unburned gas regions. Each region has its own temperature and chemical composition with the in-cylinder pressure treated as uniform throughout. It is assumed that no heat transfer occurs between the two zones and that the gases are ideal. Heat is transferred to the cylinder walls, piston and head surfaces using the Woschni[16] heat transfer model. The three zone entrainment model by Blizard and Keck[17] is employed to model flame propagation. Fresh gas is first entrained into the flame at a rate

$$\frac{dm_e}{dt} = \rho_u A_{fe} u_{te} \qquad (1)$$

where m_e is the mass of gas entrained into the flame brush, ρ_u is the unburned gas density, A_{fe} is the flame surface area and u_{te} is the turbulent entrainment burning velocity. The rate of mass burned is related to the mass entrained by

$$\frac{dm_b}{dt} = \frac{m_e - m_b}{\tau_b} \qquad (2)$$

where m_b is the mass burned and τ_b is the characteristic burn up time, calculated by

$$\tau_b = C_{\tau b} \frac{L}{u_l} \qquad (3)$$

where $C_{\tau b}$ is a model constant, L is the eddy length scale and u_l is the laminar burning velocity. The laminar burning velocity model uses the Rhodes and Keck[18] correlation. In comparison, commercial codes such as GT-Power, Ricardo Wave and AVL Boost do not distinguish between the different zones within the combustion chamber and use a single Wiebe function[19] to calculate the mass fraction of burned gas. The problems associated with the Wiebe model are that it contains no physical representation of the processes that occur during combustion and the parameters within the function

require tuning to match the burn profile for each simulation.

Our model uses the Zimont[20] turbulent burning velocity model and its associated flame development factor which was first derived by Lipatnikov and Chomiak[21] including a modification to capture the thermal expansion effects of the flame. This is achieved by multiplying the original Zimont model by a density ratio and was first used by Conway[22] and Khan[23]

$$u_{t,\infty} = C_{ut} u' Da^{1/4} \frac{\rho_u}{\rho_b} \qquad (4)$$

where $u_{t,\infty}$ is the fully developed turbulent burning velocity, u' is the turbulent RMS velocity, ρ_b is the density of the burned gas, Da is the Damköhler number and C_{ut} is a second model constant. LUSIE has been validated for the homogeneous case for numerous engines under various running conditions.[10,22–25]

The turbulence parameters (crank resolved integral length scale and turbulent RMS velocity) were generated using CFD simulations at Imperial College London. The simulations of the Jaguar Land Rover single-cylinder research engine (SCRE) were undertaken using the commercial STAR-CD/es-ice code. The code was used to simulate gas exchange and in-cylinder flow motion. The model consisted of 2.2 million cells at bottom dead centre (BDC) including the intake and exhaust ports. Time-dependent pressure and constant temperature were applied at the intake and exhaust boundaries of the model for each operating point taken from the experimental data. The base timestep used for the simulations was 0.05 °CA, which was reduced by half during the opening and closing of the valves. Turbulence was modelled using the *k*-epsilon renormalized group (RNG) model.[26,27] The turbulence parameters provided for this study were timestep resolved. The complete methodology was validated using an extensive experimental database from an old specification Jaguar Land Rover Ingenium optical engine,[28–34] and the thermodynamic SCRE used in this study. Validation results are not presented here for brevity but have been summarised by Kountouriotis.[35]

Fuel stratification modelling

The combustion process in a stratified engine starts with a spark discharge of significant duration, which therefore raises the possibility of it interacting with the fuel cloud that has developed near the spark plug. The flame kernel propagates through a highly inhomogeneous mixture spreading downstream of the rich charge to the continuously leaner mixture. As the fuel mixture is inhomogeneous, the equivalence ratio varies in both space and time. The inhomogeneous premixed combustion is the primary contributor to the heat with the non-premixed after-burning of the lean and rich mixture contributing a small amount to the heat release.[36] For the inhomogeneous premixed combustion, the local zone structure resembles the homogeneous premixed combustion but the local burning rate fluctuates according to changes in the fuel–air equivalence ratio.[37]

Since LUSIE is a quasi-dimensional thermodynamic code, it is not possible to incorporate a full three-dimensional (3D) sub-model of fuel injection. The changing fuel–air equivalence ratio, ϕ, was therefore modelled as a distribution that changes radially inside the combustion chamber using the following assumptions regarding the fuel injection process: (1) at the end of injection (EOI), the fuel stratification has some profile given by a function $\phi(r,0)$, and (2) turbulence mixes the charge, making it more homogeneous over time. To obtain a realistic model, the initial equivalence ratio distribution needs to be realistic and the effect of burned gas expansion has to be taken into account. Using a distribution like this allows for the modelling of air-, spray- and wall-guided stratification, as long as the distribution is an accurate representation at the point of ignition.

Experiments have shown that the variation in the individual-cycle fuel distributions in stratified charge engines are highly stochastic due to the turbulent in-cylinder environment which will increase cyclic variations.[38–42] Instability of the combustion is governed by convective flow fluctuations, which can prevent the flame kernel from propagating into the main stratified fuel cloud while allowing the fuel cloud to lean out due to transport and mixing.[43] Lean flame quenching then occurs at the edges of the fuel cloud.[1,44]

The equivalence ratio in our model is updated at each time step and fed into the laminar burning velocity model. Currently, the code will simply abort under extremely lean conditions as parameters do not converge, indicating to the user that combustion has not been completed. A modification of the model to include a realistic representation of flame quenching in very lean mixtures would be an interesting direction for future research.

A possible solution would be to use the Karlovitz stretch factor as a boundary at which quenching occurs. For fuels with positive stretch rate Markstein numbers, quenching has been found to occur at K≈0.8[45]

$$K \propto \frac{1}{u_l^2(\phi)} \qquad (5)$$

The relation in equation (5) shows that as the laminar burning velocity decreases, the Karlovitz stretch factor increases, and the laminar burning velocity will become small as the mixture becomes leaner, thus predicting quenching.

Equivalence ratio distribution

The radial stratified charge was incorporated into the three zone combustion models within LUSIE. The model assumes that the flame propagates from a central point of ignition, where the mixture is rich, towards the cylinder walls where the mixture becomes leaner.

Because the model is quasi-dimensional, the only point in space that can be observed is the radius of the flame at the current time step. Therefore, the model uses an initial distribution of equivalence ratio which is a function of the flame radius. The changing equivalence ratio is then passed on to the required functions and subroutines within LUSIE.

Burned gas expansion

A memory effect of stratification, which allows for a leaner mixture to burn past the lean limit when the burning followed the burning of a rich mixture, has been observed experimentally.[46] This memory effect is possibly explained by the burned gas expansion. As the volume of the burned gas increases, the expansion of this gas pushes the unburned gas, of a given equivalence ratio, closer to the cylinder walls. This means that the initial equivalence ratio profile is altered by this expansion effect at each time step. How far the gas is translated in space can be expressed as

$$\text{Translation} = r' - r \tag{6}$$

where r' is the location of an infinitesimal annular mass element of unburned gas after the burned gas expansion and r is the location of the annular element before displacement.

For a spherically propagating flame in a cylindrical combustion chamber, the volume of the unburned gas before expansion is

$$V_{u1} = \pi r^2 h - V_{b1} \tag{7}$$

where V_{u1} is the volume of unburned gas between the burned gas radius and an arbitrary point in the unburned gas at radius r. The subscript 1 denotes before expansion. V_{b1} is the volume of burned gas before expansion and h is the swept height of the cylinder. The volume of unburned gas after expansion is

$$V_{u2} = \pi r'^2 h - V_{b2} \tag{8}$$

where V_{u2} is the volume of unburned gas between the burned gas radius and a point in the unburned gas at radius, r'. The subscript 2 denotes after expansion, where V_{b2} is the volume of burned gas after expansion. Using the assumption that pressure and temperature of the unburned gas are spatially uniform and applying the ideal gas law, a relation between the volumes can be derived

$$\frac{V_{t2u}}{V_{t1u}} = \frac{V_{u2}(r')}{V_{u1}(r)} \tag{9}$$

where V_{t1u} is the total volume of unburned gas before expansion and V_{t2u} is the total volume of unburned gas after expansion. The unburned gas as a function of the radius then reads

$$\frac{\pi R^2 h - V_{b2}}{\pi R^2 h - V_{b1}} = \frac{\pi r'^2 h - V_{b2}}{\pi r^2 h - V_{b1}} \tag{10}$$

where R is the cylinder radius. Rearranging for r and r' yields

$$r = \left[\frac{V_{b1}}{\pi \cdot h} + \frac{(\pi r'^2 h - V_{b2}) \cdot (\pi R^2 h - V_{b1})}{\pi h (\pi R^2 h - V_{b2})}\right]^{\frac{1}{2}} \tag{11}$$

and

$$r' = \left[\frac{V_{b2}}{\pi \cdot h} + \frac{(\pi r^2 h - V_{b1}) \cdot (\pi R^2 h - V_{b2})}{\pi h (\pi R^2 h - V_{b1})}\right]^{\frac{1}{2}} \tag{12}$$

Turbulent mixing

The fuel–air mixture for stratified charge varies temporally as well as spatially. After the point of injection, the fuel and air are mixing together due to turbulent diffusion. The simplest way to model the effect of turbulent mixing was to use the one-dimensional diffusion equation using a turbulent diffusivity value D_t[47]

$$\frac{\partial \phi(r, t)}{\partial t} = D_t \frac{\partial^2 \phi(r, t)}{\partial r^2} \tag{13}$$

The following boundary conditions were used to determine a solution to equation (13)

$$0 \leqslant r \leqslant L \tag{14a}$$

$$\frac{\partial \phi(0, t)}{\partial r} = 0 \tag{14b}$$

$$\frac{\partial \phi(L, t)}{\partial r} = 0 \tag{14c}$$

These boundary conditions were determined from experimental equivalence ratio profiles.[14,15] Equation (14a) is derived from the charge varying radially outward from a central point at $x = 0$ to the cylinder walls at $x = L$. The boundary conditions allow for an analytical solution to be determined

$$\phi(r, t) = \phi_{eq} + A_n \cdot e^{-D_t k_n^2 t} \cdot \cos(k_n \cdot r) \tag{15}$$

where k_n is

$$k_n = \frac{\pi}{L} \tag{16}$$

and the equilibrium equivalence ratio ϕ_{eq} is

$$\phi_{eq} = \frac{\phi_{max} + \phi_{min}}{2} \tag{17}$$

While the initial distribution in space may match experimental and CFD data, the turbulent diffusivity D_t must also be realistic to correctly model how the distribution changes in time. The turbulent diffusivity is given by[48,49]

$$D_{t,\infty} = \frac{C_\mu}{Sc_t} \cdot \frac{k^2}{\varepsilon} \tag{18}$$

where k and ε are the kinetic energy and turbulent dissipation, and Sc_t and C_μ are the turbulent Schmidt number and a user defined constant, respectively. The parameters in equation (18) need to be linked to values that are obtainable in the LUSIE model. The turbulent kinetic energy can be expressed in terms of the turbulent RMS velocity

$$k = \frac{1}{2}\left(u_x'^2 + u_y'^2 + u_z'^2\right) \tag{19}$$

Due to the constraints of the quasi-dimensional model isotropic turbulence is assumed so that

$$k = \frac{3}{2}u'^2 \tag{20}$$

Consequently, the model cannot directly account for the coherent motions, swirl and tumble, that can prohibit/encourage mixing, respectively.[50] The turbulent dissipation can be written in terms of the turbulent kinetic energy and therefore is also a function of the turbulent RMS velocity

$$\varepsilon = C_\mu^{\frac{3}{4}} \cdot \left(\frac{3}{2}u'^2\right)^{\frac{3}{2}} \cdot L^{-1} \tag{21}$$

Substituting equations (20) and (21) into equation (18) gives

$$D_{t,\infty} = \frac{\sqrt{6}}{2} \cdot \frac{C_\mu^{\frac{1}{4}}}{Sc_t} \cdot u' \cdot L \tag{22}$$

where L is integral length scale when applied to the flame brush thickness in the flame speed closure (FSC) model.[4] Here, the length scale used for L is the cylinder radius.

Experimental setup

The SCRE used throughout the study was a 1-cylinder version of the latest Jaguar Land Rover gasoline Ingenium engine (Figure 1). The engine was installed at Imperial College London. A geometrical specification of the SCRE is shown in Table 1. The crankcase and bottom end of this engine took the form of a Ricardo Hydra with the valvetrain consisting of a continuously variable valve lift (CVVL) electro-hydraulic system coupled with dual-independent cam-phasing on both intake and exhaust camshafts. The CVVL unit allowed for independent control of both intake valves, therefore allowing for very different valve lift profiles including the ability to close one valve independent of the other.

Fuel mass flow measurements were taken using a Siemens SITRANS M2100 coriolis metre (accuracy of 0.1% of full scale mass flow) with airflow measurement recorded using a Labcell Laminar Flow Element (accurate to 1% of full scale mass flow). Engine out emissions, exhaust gas residuals (EGR) and air–fuel ratio (AFR) were measured using a HORIBA MEXA-ONE emissions analyser.
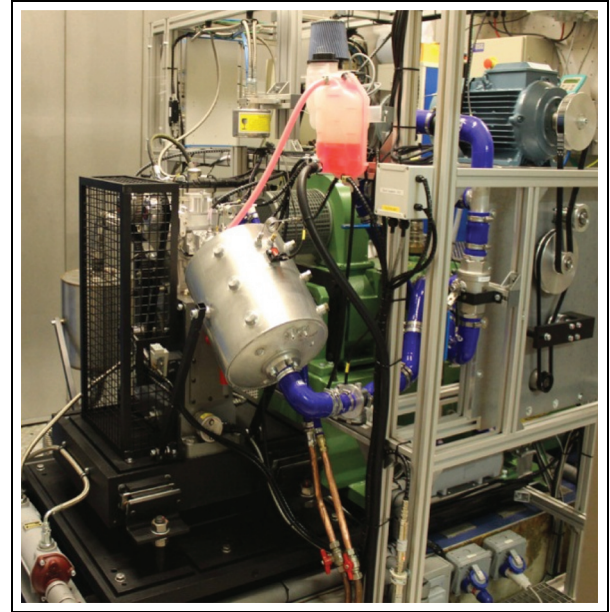

Figure 1. Jaguar Land Rover test engine.

Table 1. Jaguar Land Rover SCRE specification.

Parameter	Value
Displaced volume (cc)	499.02
Compression ratio	10.86
Number of cylinders	1
Number of valves	4
Fuel injection	Central DI
Intake maximum opening point (°CA aTDCgx)	161
Exhaust maximum opening point (°CA bTDCgx)	121
Intake phaser range (°CA)	50
Exhaust phaser range (°CA)	50

SCRE: single-cylinder research engine; DI: direct injection.

High-speed, crank angle resolved data were recorded using AVL Indicom v2.6 as part of an AVL Indiset Advanced Gigabit unit utilising a 14-bit analogue-to-digital convertor (maximum error of ±0.95, ±0.061 and ±0.122 KPa for the in-cylinder, intake and exhaust pressure channels). A water-cooled Kistler 6041B piezo-electric sensor (accurate to < 1% of full scale), mounted flush with the combustion chamber surface, in combination with a Kistler 5064 charge amplifier were used to measure in-cylinder pressure. This dynamic pressure was referenced to the intake manifold pressure (measured using a Kistler 4007 type sensor in conjunction with a Kistler 4665 signal conditioner) measured at the crank angle equidistant between the crank angles of maximum valve lift and intake valve closure. Dynamic exhaust pressure was measured using a water-cooled Kistler 4075 sensor connected to a Kistler 4665 signal conditioner. The determination of top dead centre (TDC) (accurate to 0.1 °CA) was recorded using an AVL 428 TDC sensor in combination with an AVL 365C shaft encoder operating at 720

Table 2. Exhaust gas data.

Parameter	Homogeneous	Stratified
Exhaust temperature (°C)	461	507
NOx flow (g/h)	23	12.5
CO flow (g/h)	56	130
CO_2 flow (g/h)	1800	1822
O_2 flow (g/h)	51.5	118

pulses per revolution. In-cylinder pressure was recorded at a frequency of 90 kHz at 1500 r/min; equivalent to 0.1 °CA increments. Intake and exhaust pressures were logged at one-fifth of this rate (crank angle resolution of 0.5 °CA).

Heat release metrics from combustion were calculated according to the first law of thermodynamics.[51] The polytropic coefficients for compression and expansion were calculated for each given cycle and applied to the heat release calculation in order to accurately quantify the rates of heat release irrespective of the mixture composition. The polytropic coefficient for compression was calculated from the logP versus logV diagram between the crank angles of the midpoint of intake valve closing (IVC) to ignition (start) and ignition (end); this method was adopted from the work published by Ball et al.[52] and Stone and Green-Armytage.[53] The polytropic coefficient of expansion was duly calculated from the crank angle of maximum cylinder pressure to 60 °CA aTDCf.

Indicated combustion metrics shown in the currently reported figures in the following sections were calculated for each engine cycle, with the corresponding metric from each cycle passed across to the testbed data logging software in this case DaTAQ Pro as part of a Dynamometer Services Group (DSG) testbed. Here, the instantaneous indicated data (in conjunction with testbed pressures, temperatures, mass flows and emissions measurements) were logged over a 60-s period with an average value recorded. This process was repeated twice with the three average testbed logs averaged once more to provide a single number for a given metric.

To confirm that the experimental data were stratified the exhaust gas temperatures and emissions were compared to the homogeneous case, as no optical data were available. The exhaust data are shown in Table 2, where NOx is nitrogen oxides, CO is carbon monoxide, CO_2 is carbon dioxide and O_2 is oxygen.

The increase in CO when compared to the homogeneous case is indicative of incomplete combustion associated with a stratified charge.[54] This poor combustion also leads to the excess O_2 found in the exhaust. The NOx flow has decreased for the stratified case, which could be attributed to operating at near stoichiometric conditions as well as using a high activity chamber, resulting in a relatively lean mixture as opposed to an extremely lean mixture/air near the walls.
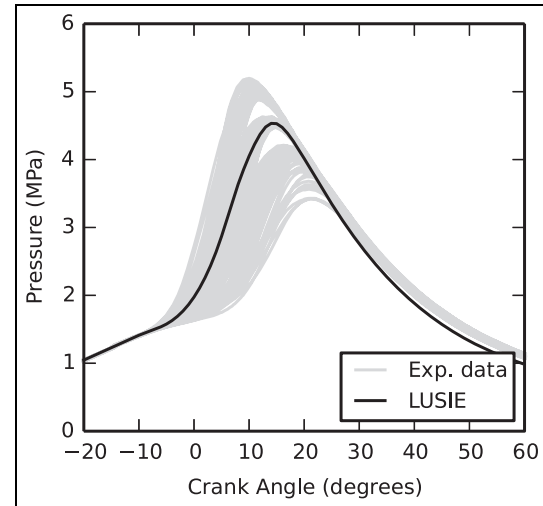

Figure 2. LUSIE simulated crank-resolved pressure trace with tuned constants and experimental data at 1500 r/min and GMEP of 0.79 MPa.

Validation

Homogeneous validation

LUSIE has previously been validated for homogeneous combustion in very different types of gasoline engines compared to the one used in this study. Therefore, we begin by validating the model for homogeneous combustion in the specific engine used in this study.

The validation is a two-step process where the model constants are first tuned so that simulations match the pressure trace for a selected set of running conditions. Then, to demonstrate that the model has predictive capabilities, it is run under different initial conditions using the constants determined for the tuned case shown in Figure 2. The running conditions for the tuned and predicted cases are shown in Table 3 with P_{int} being the in-cylinder pressure at IVC, T_{int} the in-cylinder temperature at IVC and GMEP is the gross mean effective pressure.

The experimental data consisted of 300 cycles for each running condition. These data were then divided into fast, middle and slow combustion cycles while removing data in-between these regions. This approach is commonly used when dealing with cyclic variability.[22,24,55] Fast, middle and slow cycle are determined by the peak pressure values, with the fast combustion cycles defined as $P_{max} \geqslant \bar{P}_{max} + \sigma$, where $\bar{P}_{max}$ is the mean peak pressure value and σ is the standard deviation. The middle cycles are defined as $\bar{P}_{max} - 0.25\sigma \leqslant P_{max} \leqslant \bar{P}_{max} + 0.25\sigma$. Finally, slow cycles are defined as $P_{max} \leqslant \bar{P}_{max} - \sigma$.

In the three-zone entrainment model, the burn-up time constant $C_{\tau b}$ in equation (3) has been found to change from engine to engine.[22] It is tuned to simulate a middle engine cycle. A value of $C_{\tau b} = 9$ was found to be reasonable when the eddy length scale L is set to the Taylor micro-scale of turbulence. Another model

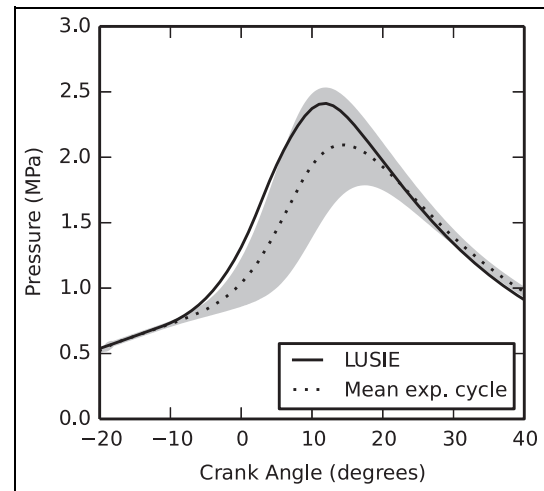**Table 3.** Running conditions for homogeneous case validation.

Parameter	Tuned	Predicted
Engine speed (r/min)	1500	1500
P_{int} (MPa)	0.135	0.07
T_{int} (K)	388.8	403.2
Spark advance (° aTDC)	−15.0	−20.0
Throttle	Wide open	Throttled
Engine load (GMEP) (MPa)	0.79	0.36

GMEP: gross mean effective pressure.
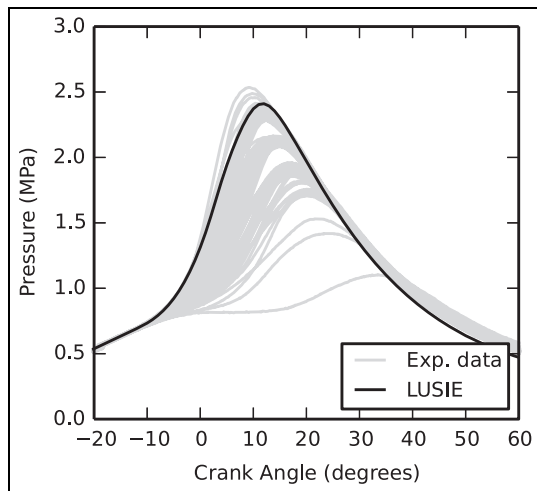
Figure 3. LUSIE simulated crank-resolved pressure trace, with model constants determined from Figure 2, and experimental data at 1500 r/min and GMEP of 0.36 MPa.

Figure 4. LUSIE simulated crank-resolved pressure trace, mean experimental cycle and 95% confidence interval at 1500 r/min and GMEP of 0.36 MPa.

constant, C_{ut}, in the modified Zimont–Lipatnikov model equation (4), also required tuning. A value of 0.35 was found to reasonable for both naturally aspirated and turbo-charged engines[22] and was used throughout the work presented here. A comparison of the tuned pressure trace to experimental data is shown in Figure 2. The simulation shows good agreement with the experimental data and represents a middle combustion cycle.

The simulated pressure trace for the predicted case in Figure 3 falls within the experimental bounds. Simulated results also fall largely into the 95% confidence interval (grey area) of the experimental data as shown in Figure 4. However, during the early stages of combustion, the predicted cycle is on the border of the 95% confidence interval, showing that LUSIE is predicting values for the fastest 2.5% of cycles there. In contrast to the tuned case, the simulation is no longer representative of the middle cycles, but of faster combustion cycles. Preliminary results have shown for the unthrottled tuned case, shown in Figure 2, that the equivalence ratio in the vicinity of the spark is inhomogeneous with an average value leaner than stoichiometric. This has been accounted for in the tuned case by increasing the spark delay time, where the spark delay time is the time taken for a spark kernel of a given size to form after the point of ignition. For the throttled case shown in Figures 3 and 4, the mixture may be even leaner meaning that the spark delay time would need increasing, thus reducing the speed and peak pressure of combustion making the simulation a closer representative of a middle cycle. Further research on the spray formation in the vicinity of the spark is required.

Stratified validation

The initial conditions for the experimental stratified case are the same as those stated for the homogeneous predicted case in Table 3, the exception being the fuel injection timing. The EOI for homogeneous combustion (Figures 2 and 3) was 293° before top dead centre (bTDC), whereas the EOI for stratified combustion was 43 °bTDC. For the simulated stratified case, the maximum equivalence ratio was set to 1.28 and the minimum equivalence ratio set to 0.68. The minimum equivalence ratio was chosen as 0.68 as the engine has a high activity chamber, meaning that the charge near the walls would not be as lean as is usually associated with a stratified charge. The maximum equivalence ratio was selected to ensure that the average equivalence ratio was equal the average experimental equivalence ratio for the stratified case. Due to a lack of any optical data, both the minimum and maximum equivalence ratios are weakly constrained and subject to substantial uncertainty; however, results were relatively robust, with variations of ±10% still being well within experimental bounds.

Compared in Figure 5 are the crank-resolved pressure profiles for the simulated and experimental stratified case.

The simulated stratified charge is in good agreement with the experimental case, falling well within the 95%
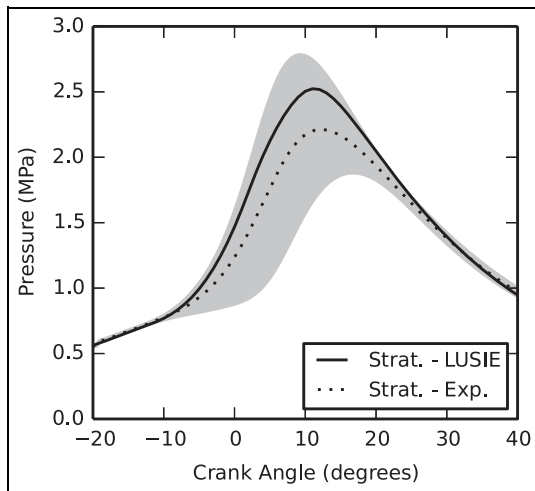
Figure 5. LUSIE simulated crank-resolved pressure trace, mean experimental cycle and 95% confidence interval for the stratified case at 1500 r/min and GMEP of 0.36 MPa.

Figure 6. Percentage heat release for the simulated and experimental case under stratified conditions at 1500 r/min and GMEP of 0.36 MPa.

confidence interval. Like the predicted homogeneous case, the stratified model also simulates a fast cycle under throttled running conditions. The difference in peak pressure (ΔP_{max}) and location of peak pressure (ΔP_θ) between the stratified and homogeneous experimental mean cycles is 0.118 MPa and $-2.2°$, respectively. This shows that the stratified case has a greater peak pressure value which occurs earlier than the homogeneous case. For the simulated case ΔP_{max} equals 0.113 MPa and ΔP_θ equals $-1°$. The model thus captures the mild increase in peak pressure due to stratification with a high degree of accuracy. However, its performance is weaker in representing the difference in the point at which the peak value occurs. This could be due to a slower burning velocity, as a result of a smaller predicted equivalence ratio leading to a later peak pressure value.

To illustrate the importance of modelling turbulent mixing of the stratified charge, simulations were also undertaken with the mixing model switched off. These led to a ΔP_{max} value of 0.173 MPa lower, and a ΔP_θ value of $0°$ compared to the homogeneous case. Without turbulent mixing, the stratified model therefore predicts a decrease in peak pressure from stratification in contrast to what is seen in experiments and fails to detect a change in peak pressure position. Turbulent mixing is therefore important to include when modelling stratified combustion.

As a second point of validation for the model, the rate of heat release was also compared to experimentally obtained data. The heat release for the simulated case was calculated using normalised mass fraction burned with respect to the maximum mass fraction burned value, due to the incomplete combustion of the mixture for the stratified case. For both the tuned and predicted homogeneous cases (not shown), the modelled rate of heat release fell within experimental
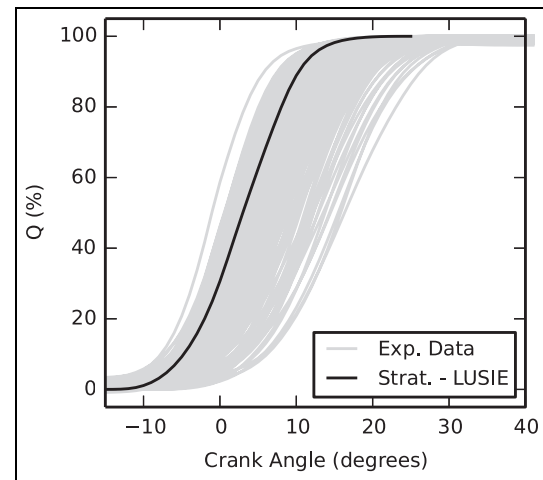
bounds. Compared in Figure 6 are the rate of heat release for the modelled and experimental cases for stratified conditions. In line with the pressure trace shown in Figure 5, the percentage heat released for stratified conditions tends towards the fast combustion cycles but falls well within the experimental bounds. It is worth stressing that no further tuning of the model parameters was required beyond the initial tuning shown in Figure 2.

Conclusion

Presented in this article is a quasi-dimensional stratified charge model for SI engines containing three physical sub-models: (1) equivalence ratio distribution, (2) burned gas expansion and (3) turbulent mixing. It was then used to validate the stratified fuel model against experimental data for both the in-cylinder pressure trace and rate of heat release. For both the in-cylinder pressure and heat release, the model fell within experimental bounds representing a fast combustion cycle. The effect of turbulent mixing was also investigated. The trend between the stratified and homogeneous simulations matched closest to the experimental data for when the mixing model was included when comparing the parameters ΔP_{max} and ΔP_θ. The simulations where mixing was not used for the stratified case actually showed the opposite trend to the experimental data.

ORCID iDs

Jamie Karl Smith (iD) https://orcid.org/0000-0001-6295-799X
Daniel Ruprecht (iD) https://orcid.org/0000-0003-1904-2473

References

1. Zhao F, Lai MC and Harrington DL. Automotive spark-ignited direct-injection gasoline engines. *Prog Energ Combust* 1999; 25(5): 437–562.
2. Schmieg SJ. Aspects of HC-SCR catalyst durability for lean-burn engine exhaust aftertreatment. *SAE Inter J Fuels Lubr* 2010; 3(2): 691–709.
3. Wirth M, Piock WF, Fraidl GK, Schoeggl P and Winkl-hofer E. Gasoline DI engines: the complete system approach by interaction of advanced development tools. SAE technical paper 980492, 1998.
4. Huang C, Lipatnikov A, Johansen LCR and Hemdal S. A study of two basic issues relevant to RANS simulations of stratified turbulent combustion in a spray-guided direct-injection spark-ignition engine. SAE technical paper 2014-01-2572, 2014.
5. Huang C, Yasari E and Lipatnikov A. A numerical study on stratified turbulent combustion in a direct-injection spark-ignition gasoline engine using an open-source code. SAE technical paper 2014-01-1126, 2014.
6. Huang C, Yasari E, Johansen LCR, Hemdal S and Lipatnikov A. Application of flame speed closure model to RANS simulations of stratified turbulent combustion in a gasoline direct-injection spark-ignition engine. *Combust Sci Technol* 2016; 188(1): 98–131.
7. Liu J, Gong J, Cai L, Tan L, Ni X and Gao W. Multi-dimensional simulation of air/fuel premixing and strati-fied combustion in a gasoline direct injection engine with combustion chamber bowl offset. SAE technical paper 2006-32-0006, 2006.
8. Duclos J and Zolver M. 3D modeling of intake, injection and combustion in a DI-SI engine under homogeneous and stratified operating conditions. In: *Fourth international symposium COMODIA*, 20–23 July 1998, Kyoto, Japan, vol. 98, pp.335–340.
9. Gong C, Peng L and Liu F. Modeling of the overall equivalence ratio effects on combustion process and unregulated emissions of an SIDI methanol engine. *Energy* 2017; 125: 118–126.
10. Aghdam EA. *Improvement and validation of a thermodynamic S.I. engine simulation code*. PhD Thesis, University of Leeds, Leeds, 2003.
11. Schmid A, Grill M, Berner HJ and Böttcher M. Development of a quasi-dimensional combustion model for stratified SI-engines. SAE technical paper 2009-01-2659, 2009.
12. Sjeric M, Kozarac D and Sagi G. Development of a stratified fractal combustion model. In: *XXIII JUMV international automotive conference 'science and motor vehicles'*, Belgrade, Serbia, 19–21 April 2011.
13. Aliramezani M, Chitsaz I and Mozafari AA. Thermodynamic modeling of partially stratified charge engine characteristics for hydrogen-methane blends at ultra-lean conditions. *Int J Hydrogen Energ* 2013; 38(25): 10640–10647.
14. Moriyoshi Y, Morikawa H, Kamimoto T and Hayashi T. Combustion enhancement of very lean premixture part in stratified charge conditions. SAE technical paper 962087, 1996.
15. Moriyoshi Y, Morikawa H and Komatsu E. Analysis of turbulent combustion in simplified stratified charge conditions. *JSME Int J, Series B: Fluid Therm Eng* 2003; 46(1): 86–91.
16. Woschni G. A universally applicable equation for the instantaneous heat transfer coefficient in the internal combustion engine. SAE technical paper 670931, 1967.
17. Blizard NC and Keck JC. Experimental and theoretical investigation of turbulent burning model for internal combustion engines. SAE technical paper 740191, 1974.
18. Rhodes DB and Keck JC. Laminar burning speed measurements of indolene-air-diluent mixtures at high pressures and temperatures. SAE technical paper 850047, 1985.
19. Vibe I. *Halbempirishe formel dur die verbrennungsgeschwindigkeit*. New York: Springer Verlag, 1964, pp.156–159.
20. Zimont V. Theory of turbulent combustion of a homogeneous fuel mixture at high Reynolds numbers. *Combust Explo Shock +* 1979; 15: 305–311.
21. Lipatnikov AN and Chomiak J. A simple model of unsteady turbulent flame propagation. SAE technical paper 972993, 1997.
22. Conway G. *Cyclic variability of flame propagation and autoignition in supercharged and naturally aspirated SI engines*. Thesis, University of Leeds, Leeds, 2013.
23. Khan AF. *Chemical kinetics modelling of combustion processes in SI engines*. Thesis, University of Leeds, Leeds, 2014.
24. Abdi Aghdam E, Burluka AA, Hattrell T, Liu K, Sheppard CGW, Neumeister J and Crundwell N. Study of cyclic variation in an SI engine using quasi-dimensional combustion model. SAE technical paper 2007-01-0939, 2007.
25. Hattrell T. *A computational and experimental study of spark ignition engine combustion*. Thesis, University of Leeds, Leeds, 2007.
26. Yakhot V and Orszag SA. Renormalization group analysis of turbulence. i. basic theory. *J Sci Comput* 1986; 1(1): 3–51.
27. Yakhot V, Orszag S, Thangam S, Gatski TB and Speziale CG. Development of turbulence models for shear flows by a double expansion technique. *Phys Fluids A: Fluid* 1992; 4(7): 1510–1520.
28. Justham T, Jarvis S, Garner CP, Hargrave GK, Clarke A and Richardson D. Single cylinder motored SI IC engine intake runner flow measurement using time resolved digital particle image velocimetry. SAE technical paper 2006-01-1043, 2006.
29. Jarvis S, Justham T, Clarke A and Richardson D. Motored SI IC engine in-cylinder flow field measurement using time resolved digital PIV for characterisation of cyclic variation. SAE technical paper 2006-01-1044, 2006.

30. Serras-Pereira J, Aleiferis PG, Richardson D and Wallace S. Characteristics of ethanol, butanol, iso-octane and gasoline sprays and combustion from a multi-hole injector in a DISI engine. *SAE Int J Fuels Lubr* 2008; 1(1): 893–909.

31. Serras-Pereira J, Aleiferis PG and Richardson D. An experimental database on the effects of single- and split injection strategies on spray formation and spark discharge in an optical direct-injection spark-ignition engine fuelled with gasoline, iso-octane and alcohols. *Int J Engine Res* 2015; 16(7): 851–896.

32. Williams B, Ewart P, Stone R, Ma H, Walmsley H, Cracknell R, et al. Multi-component quantitative PLIF: robust engineering measurements of cyclic variation in a firing spray-guided gasoline direct injection engine. SAE technical paper 2008-01-1073, 2008.

33. Williams B, Ewart P, Wang X, Stone R, Ma H, Walmsley H, et al. Quantitative planar laser-induced fluorescence imaging of multi-component fuel/air mixing in a firing gasoline-direct-injection engine: effects of residual exhaust gas on quantitative PLIF. *Combust Flame* 2010; 157(10): 1866–1878.

34. Serras-Pereira J, Aleiferis PG and Richardson D. An analysis of the combustion behavior of ethanol, butanol, iso-octane, gasoline, and methane in a direct-injection spark-ignition research engine. *Combust Sci Technol* 2013; 185(3): 484–513.

35. Kountouriotis A. Thesis in preparation, Imperial College London, 2018.

36. Lipatnikov A. *Fundamentals of premixed turbulent combustion*, vol. 1. Boca Raton, FL: CRC Press, 2012.

37. Bilger RW, Pope SB, Bray KNC and Driscoll JF. Paradigms in turbulent combustion research. *P Combust Inst* 2005; 30(1): 21–42.

38. Ghandi JB, Felton PG, Gajdeczko BF and Bracco F. Investigation of the fuel distribution in a two-stroke engine with an air-assisted injector. SAE technical paper 940394, 1994.

39. Fansler TD, French DT and Drake MC. Fuel distributions in a firing direct-injection spark-ignition engine using laser induced fluorescence imaging. SAE technical paper 950110, 1995.

40. Ghandi JB and Bracco FV. Fuel distribution effects on the combustion of a direct-injection stratified-charge engine. SAE technical paper 950460, 1995.

41. Drake MC, French DT and Fansler TD. Advanced diagnostics for minimizing hydrocarbon emissions from a direct-injection gasoline engine. *P Combust Inst* 1996; 26(2): 2581–2587.

42. Ghandi JB and Bracco FV. Mixture preparation effects on ignition and combustion in a direct-injection spark-ignition engine. SAE technical paper 962013, 1996.

43. Fansler TD, Reuss DL, Sick V and Dahms RN. Combustion instability in spray-guided stratified-charge engines: a review. *Int J Engine Res* 2015; 16(3): 260–305.

44. Fansler TD and Drake MC. Flow, mixture preparation and combustion in direct-injection two-stroke gasoline engines. In: Arcoumanis C and Kamimoto T (eds) *Flow and combustion in reciprocating engines*. Heidelberg: Springer-Verlag, 2009, pp.67–136.

45. Bradley D, Lawes M, Liu K and Mansour MS. Measurements and correlations of turbulent burning velocities over wide ranges of fuels and elevated pressures. *P Combust Inst* 2013; 34(1): 1519–1526.

46. Balusamy S, Cessou A and Lecordier B. Laminar propagation of lean premixed flames ignited in stratified mixture. *Combust Flame* 2014; 161(2): 427–437.

47. Tennekes H and Lumley JL. *A first course in turbulence*. Cambridge, MA: MIT Press, 1972.

48. Launder BE and Spalding DB. *Mathematical models of turbulence*. London: Academic Press, 1972.

49. Hill PG and Zhang D. The effects of swirl and tumble on combustion in spark-ignition engines. *Prog Energ Combust* 1994; 20(5): 373–429.

50. Berckmüller M, Tait NP and Greenhalgh DA. The time history of the mixture formation process in a lean burn stratified-charge engine. SAE 961929, 1996.

51. Stone R. *Introduction to internal combustion engines*. Palgrave Macmillan, Basingstoke, UK, 2012.

52. Ball J, Raine R and Stone C. Combustion analysis and cycle-by-cycle variations in spark ignition engine combustion part 2: a new parameter for completeness of combustion and its use in modelling cycle-by-cycle variations in combustion. *Proc IMechE, Part D: J Automobile Engineering* 1998; 212(6): 507–523.

53. Stone CR and Green-Armytage DI. Comparison of methods for the calculation of mass fraction burnt from engine pressure–time diagrams. *Proc IMechE, Part D: J Automobile Engineering* 1987; 201(1): 61–67.

54. Lumley JL. *Engines: an introduction*. Cambridge: Cambridge University Press, 1999.

55. Burluka AA, El-Dein Hussin AMTA, Ling ZY and Sheppard CGW. Effects of large-scale turbulence on cyclic variability in spark-ignition engine. *Exp Therm Fluid Sci* 2012; 43: 13–22.